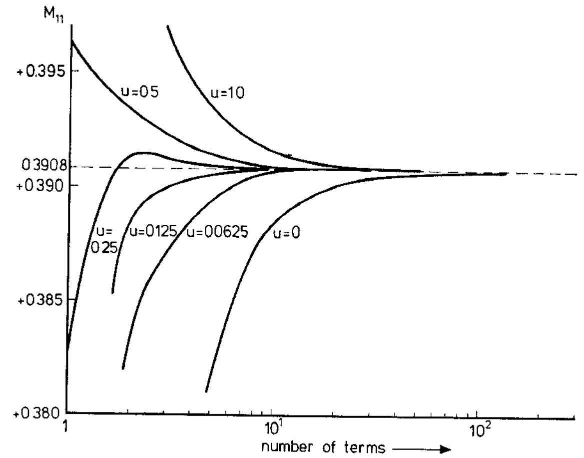

Fig. 1. Matrix element M_{11} as a function of number of terms in the series.

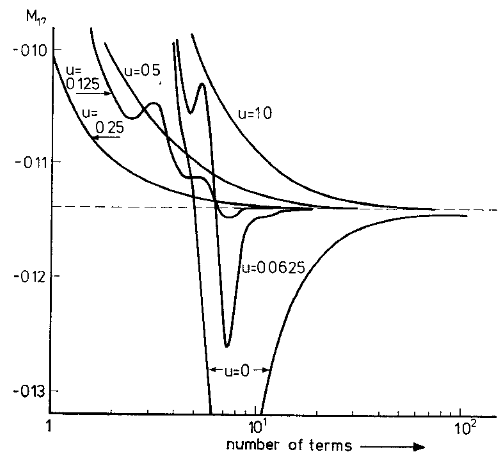

Fig. 2. Matrix element M_{17}.

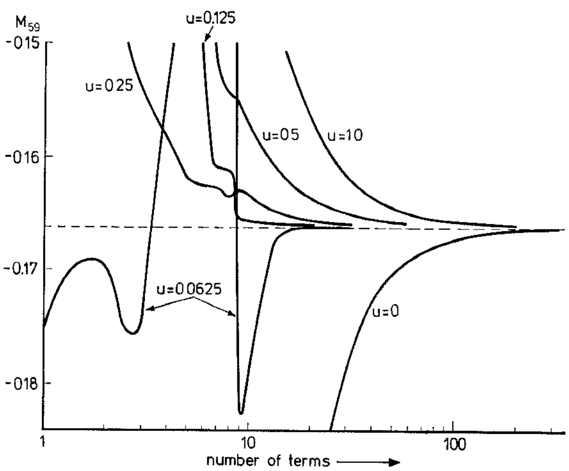

Fig. 3. Matrix element M_{59}.

As an example, the matrix element M_{11} was computed for the following values of the parameters: $d/w=0.4190$ and $d/\lambda=0.3431$ by means of (4) and (9). With these dimensions, the fundamental mode of the guide is above cutoff and its contribution does not appear in the series (4). This is tantamount to taking $\Gamma_1=0$ in (9).

The results are shown in Fig. 1, where the sum of the series truncated after terms $(N=(n+1)/2)$ is plotted against N for various values of u. The curve corresponding to $u=0$ is the original series (4), as can be seen by inspection of (5) and (6).

No resonance can occur in M_{11}. An example of its occurrence is illustrated in Fig. 2, where the result of truncating the series in the matrix element M_{17} after N terms is plotted against N. For a symmetrical aperture, $k=7$ corresponds to a four-term modal development. A resonance peak appears as n approaches 17, since then $k/n=7/17\simeq 0.419=d/w$ and its contribution to the sum is only slowly compensated by that of following terms of the opposite sign. It follows that no fewer than 200 terms will be needed in order to achieve a fourth decimal accuracy. The situation deteriorates for larger values of m and k. The same accuracy is achieved after 10 terms of the modified series, with the value u set equal to 1/5 by a simple estimate.

As $u\rightarrow 0$, a resonance begins to show also in the transformed series, as it should do, by continuity. The appearance of two resonances for m and k larger than unity is illustrated in Fig. 3 ($m=5$, $k=9$).

Acknowledgment

The authors wish to thank Dr. A. Douglas for his interest and suggestions. They also wish to thank Dr. W. Mecklenbräuker and J. de Groot for their helpful discussions.

References

[1] J. Schwinger and D. Saxon, *Discontinuities in Waveguides.* London, England: Gordon and Breach, 1968, ch. III.
[2] R. E. Collin, *Field Theory of Guided Waves.* New York: McGraw-Hill, 1960, ch. 8.
[3] R. F. Harrington, *Field Computation by the Moment Method.* New York: Macmillan, 1964.
[4] S. W. Lee, W. R. Jones, and J. J. Campbell, "Convergence of numerical solutions of iris-type discontinuity problems," *IEEE Trans. Microwave Theory Tech.*, vol. MTT-19, pp. 528–536, June 1971.
[5] A. Wexler, "Solution of waveguide discontinuities by modal analysis," *IEEE Trans. Microwave Theory Tech.*, vol. MTT-15, pp. 508–517, Sept. 1967.
[6] P. Morse and H. Feshbach, *Methods of Theoretical Physics*, vol. 1. New York: McGraw-Hill, 1953, pp. 413–414.

Time-Delay Limits Set by Dispersion in Magnetostatic Delay Lines

M. BINI, L. MILLANTA, N. RUBINO, AND V. TOGNETTI

***Abstract*—Analysis and experiments show the extreme dispersion of magnetostatic delay lines. A suitable parameter to characterize the amount of dispersion present has been found to be the maximum output energy contained in a time interval equal to the input pulse duration. The time occurrence of this maximum value gives a convenient measure of the group delay. The pulse shape and energy content versus delay have been determined both theoretically and experimentally for axially magnetized circular rods. The results show that delays beyond two to three times the input pulse duration cannot be obtained with more than 50 percent of the output energy contained within the original pulse duration.**

I. Theory

The magnetostatic-wave group delay in axially magnetized ferrite rods has been expressed as [1]

$$\tau_g(\omega)=\frac{\alpha}{\omega-\omega_c} \tag{1}$$

where ω_c is the cutoff angular frequency of the volume modes and $\alpha=j_{mn}(1+q^2)^{5/4}/\sqrt{3}q^2$ [1] is a parameter taking care of the ferrite sample and the mode involved, q being the ratio of diameter to length of the rod and j_{mn} the nth root of the mth-order Bessel function. In our case we deal with the (1, 1) mode, $j_{01}=2.405$ [2]. Equation (1) assumes a parabolic internal field profile.[2]

To investigate the amount of dispersion introduced by the magnetostatic line, we want to derive the output signal corresponding to a rectangular pulse-modulated input frequency ω_0. To do this we assume a transfer function $A(\omega)\exp j\phi(\omega)$ with $A(\omega)=\text{const}=A$, and $\phi(\omega)$ approximated by a power expansion with the terms up to the

Manuscript received February 17, 1972; revised June 29, 1972.
The authors are with Consiglio Nazionale delle Ricerche, Istituto di Ricerca sulle Onde Elettromagnetiche (ex Centro Microonde), 50127 Florence, Italy.

[1] Our theory and experiments refer to two-port delay lines (input-to-output transmission) whereas [1] deals with one-port (pulse-echo) delay lines. The factor of 2 appearing in [1] is not, therefore, included here.

[2] For a more accurate computation, the Sommerfeld [3] field profile could be introduced. The improvement, however, did not show to be substantial for the commonly used aspect ratios, $q=0.2\cdots 0.3$ [4].

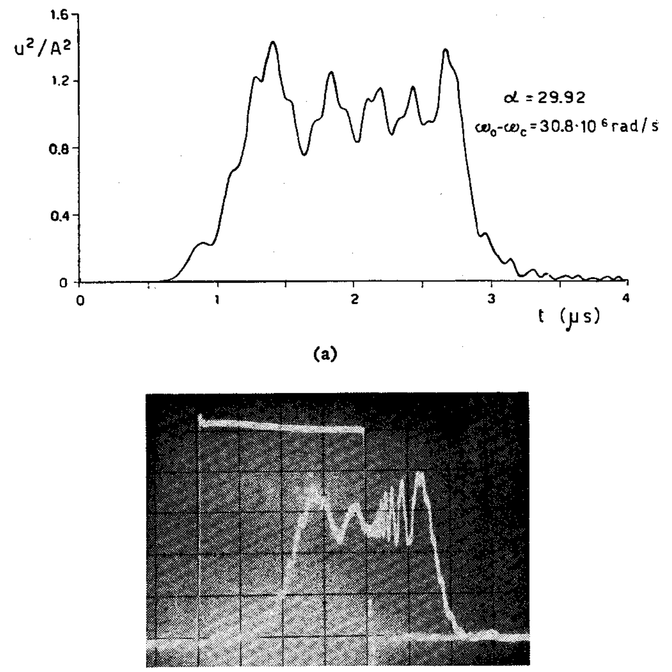

Fig. 1. (a) Computed output-signal envelope (squared). (b) Experimental output power envelope for aspect ratio $q=0.222$, mode (1, 1), and distance from cutoff as in (a). The time scale of the oscilloscope 0.5 μs/div. The fast ringing following the trailing edge of the input pulse in (b) is attributable to cutoff (not accounted for in (a)).

third order retained:

$$\phi(\omega) = \phi(\omega_0) - \tau_g(\omega_0)(\omega - \omega_0) + \frac{1}{2}\frac{\alpha}{(\omega_0 - \omega_c)^2}(\omega - \omega_0)^2 - \frac{1}{3}\frac{\alpha}{(\omega_0 - \omega_c)^3}(\omega - \omega_0)^3. \quad (2)$$

It should be noted that the above expression is meaningless for $\omega_0 \leq \omega_c$ and that the presence of the cutoff, affecting the lower frequencies of the input-signal spectrum, is ignored. The envelope of the output signal is found using the Fourier inverse transform of the transfer function given above and doing the convolution with the input signal rect (t/T) exp $(j\omega_0 t)$, where T is the input pulse duration. The output-signal envelope $u(z)$ is thus obtained with some manipulations [4]:

$$u(z) = A\,\frac{\pi^{2/3}}{p_2}\left|\int_{z-1/2}^{z+1/2} \mathrm{Ai}\left[-\frac{\pi^{2/3}}{p_2}\left(z + \frac{p_1^4}{4p_2^3}\right)\right] \cdot \exp\left[j\,\frac{\pi p_1^2}{2p_2^3}\,z\right] dz\right| \quad (3)$$

where z is a normalized time variable: $z=[t-\tau_g(\omega_0)]/T$; Ai is the Airy integral as defined in [5]; $p_1=[\tau_g(\omega_0)(\pi/\alpha)^{1/2}]/T$; $p_2=[\tau_g(\omega_0)(\pi/\alpha)^{2/3}]/T$. The parameters p_1 and p_2 take into account, respectively, the slope and the curvature of the group delay versus frequency as given by (2) ($\tau_g=-d\phi/d\omega$) with $\tau_g(\omega_0)$ given by (1). The expression (3) is in a form suitable for computation.[3] An example of the output pulse shape is given in Fig. 1(a), for a typical case. Fig. 1(a) displays the power envelope—the square of $u(z)$—rather than the amplitude envelope, for convenience of comparison with the experimentally observed pulse as detected by a square-law detector.

Given the fact that dispersion is after all energy spreading in time, a convenient quantity that we now introduce to characterize the amount of dispersion is the ratio E/E_0 where

$$E_0 = T\int_{-\infty}^{+\infty} u^2(z)dz$$

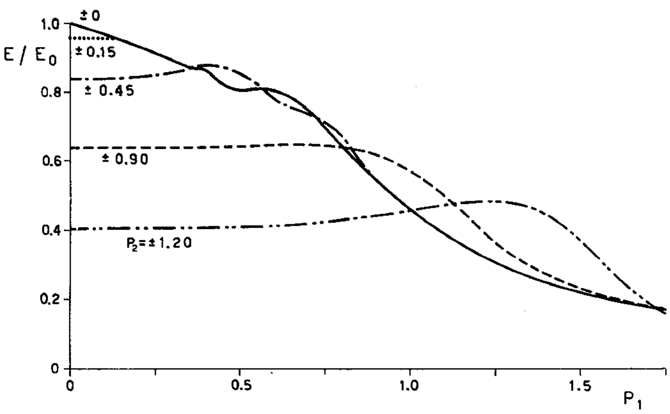

Fig. 2. Dispersion parameter E/E_0 versus p_1 for various values of p_2.

is the total output energy of the pulse and

$$E = T\int_{-1/2}^{+1/2} u^2(z)dz$$

is that fraction of the output pulse energy which is contained in a time interval T, delayed by $\tau_g(\omega_0)$ with respect to the input pulse. Curves of E/E_0 versus p_1 are shown in Fig. 2 for various values of p_2. The case $p_2=0$ is also shown (solid line). Note that when $p_2 \neq 0$, E/E_0 does not reach unity even for $p_1=0$, thus showing the presence of dispersion due to the cubic term of the phase function. From Fig. 2 one can evaluate the amount of dispersion when the line is given (given α) for a required value of time delay $\tau_g(\omega_0)$ and pulse length T.

II. Experiments and Discussion

All experiments were performed at room temperature, in the gigahertz range.[4] The shape of the pulse transmitted through the delay line—a YIG rod—was observed with a very wide-band receiver. The cutoff frequency ω_c was identified and the carrier frequency ω_0 was set at a chosen distance from cutoff. An example is shown in Fig. 1(b) and compared with the theoretical case of Fig. 1(a) corresponding to the same aspect ratio and distance from cutoff, for the (1, 1) mode. The theoretical τ_g is thus determined by (1) to be 0.975 μs and is used to set Fig. 1(a) to the proper $t=0$ reference. The transmitted pulse very far from cutoff (undelayed) is also shown (not in scale) in Fig. 1(b) for the $t=0$ reference. The delay as measured with the gate method (see below) turns out to be 1 μs. The main difference between theoretical and experimental shapes appears to be the fast ringing following immediately after the falling edge of the input pulse; the same phenomenon is also present, but less visible, after the leading edge. This discrepancy seems to be attributable to the fact that cutoff is not taken into account in this theory: a qualitative explanation due to Burke [7] assumes that the higher frequency components of the input pulse spectrum, undergoing negligible group delay, interfere with the delayed components near cutoff, in the absence of the low-frequency components which are cut off.

Measurements of energy content at the output were performed as follows. An RF pulse was formed by means of a p-i-n modulator and was sent through the YIG sample. A second p-i-n modulator (the "gate") was placed after the YIG sample and was followed by an average-reading broad-band power meter. The gate was pulsed "on" for a time duration equal to that of the incident RF pulse and its time occurrence could be varied with respect to the first pulse. The gate delay was varied until a maximum of output power was observed. This was measured and expressed as a percentage of all the power going out of the YIG under the same conditions. This gave the maximum value of the ratio E/E_0. The corresponding value of the time delay was also measured. It may be worth pointing out that this E/E_0 measurement has nothing to do with the insertion-loss measurement; mismatch and attenuation losses do not come into play, all power measurements being performed at the output.

The gate delay at maximum output does not necessarily correspond to group delay. It can be theoretically demonstrated [4] that an extreme of E/E_0 occurs at time $t=\tau_g$ when the output signal

[3] Numerical computation becomes increasingly difficult as p_2 approaches zero. When $p_2=0$, (3) loses meaning. However, the case $p_2=0$ (linear approximation of group delay versus frequency) has been already solved in terms of Fresnel integrals (see [6]).

[4] *Note added in proof:* Experiments at the liquid-He temperature were also performed later, which confirmed the delay and dispersion behavior shown in this short paper. This was expected, since losses were recognized to be of minor importance, as the time-delay limits are concerned (see Section III).

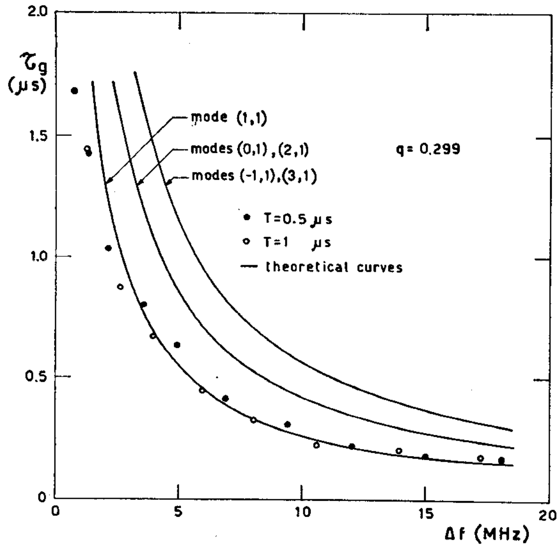

Fig. 3. Theoretical group delay (solid lines) versus frequency distance from cutoff for various modes and a given aspect ratio q. Dots are experimental values of the delay measured by the "gate" method.

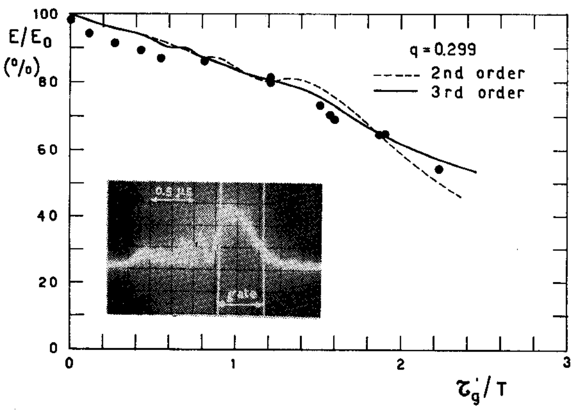

Fig. 4. Dispersion parameter E/E_0 versus reduced delay τ_g/T, for a given aspect ratio q, computed for two different approximations of (2). Dots are experimental data. The insert shows an example of pulse output when E/E_0 is 65 percent.

envelope is symmetrical, and symmetry is insured when the transfer function is symmetrical with respect to ω_0. This is, for instance, true of the linear case of footnote 3. In the case of the magnetostatic delay line, the experiments show the gate delay to closely correspond to the group delay as in the example of Fig. 3.[5] We can thus compare the theoretical results of E/E_0 at $t=\tau_g$, versus τ_g, with the measurements of (E/E_0)max versus the gate delay. This is shown in Fig. 4, where the third- and second-order approximations are both shown. The agreement between theory and experiment is satisfactory. The fact that the quadratic and cubic approximations give very similar results is true for the commonly used aspect ratios and for the quantity E/E_0 (not for the pulse shape).

From Fig. 4 we derive that even accepting an energy degradation around 50 percent, the delay is still only somewhat more than twice the pulse duration. Note that a degradation of this order appears to be rather extreme because one-half of the output energy is outside the original pulse duration. In practice a "delayed pulse" of this sort is hardly recognizable as a pulse. An example of delayed pulse corresponding to a 65-percent energy degradation is shown in the insert of Fig. 4.

Of course, using lower aspect ratios or higher modes (greater α) reduces dispersion, but the gain in delay for a given dispersion is not large, as can be derived from the α dependence of p_1 and p_2 and from Fig. 2. Computations and experiments with other aspect ratios confirm the behavior of Fig. 4 (e.g., with a $q=0.222$ and a 50-percent energy degradation the delay is still about $3T$).

[5] The excited mode was the (1, 1) mode, as indicated not only by Fig. 3, but also by previous measurements of dispersion curves [8] and by the output pulse shapes (e.g., Fig. 1).

III. Conclusions

On the basis of theoretical considerations and experiments it can be affirmed that the obtainable magnetostatic delay is limited, for normal aspect ratios, to about 3 times the pulse duration. Dispersion is the limiting factor; losses play a very minor role, as demonstrated by the fact that our theory, though lossless, agrees with the experiments satisfactorily.

Some improvement for practical signal-processing purposes might be obtained by reducing the harmonic content of the "delayed" pulse, either adopting a more suitable input pulse shape (e.g., Gaussian shape) or using suitable filtering techniques. Still, improvement amounts to a better display of the information available, not, of course, to a reduction of the transmission distortion.

Additionally, we suggest the energy degradation parameter E/E_0, as a convenient and physically meaningful parameter in dispersion problems. Also, the gate method has proved very effective for time-delay measurements in extreme dispersion situations, where leading and trailing edges, maxima, and 50-percent levels are no longer clearly identifiable.

References

[1] R. W. Damon and H. van de Vaart, "Propagation of magnetostatic spin waves at microwave frequencies, II rods," *J. Appl. Phys.*, vol. 37, p. 2445, 1966.
[2] R. I. Joseph and E. Schlömann, "Theory of magnetostatic modes in long axially magnetized cylinders," *J. Appl. Phys.*, vol. 32, p. 1001, 1961.
[3] A. Sommerfeld, *Electrodynamics*. New York: Academic Press, 1964, p. 82.
[4] M. Biri, L. Millanta, N. Rubino, and V. Tognetti, "A dispersive medium with cubic phase characteristic: Application to the magnetostatic delay line," Istituto di Ricerca sulle Onde Elettromagnetiche, Florence, Italy, Tech. Rep. 131-6-11, Jan. 1971.
[5] A. Abramowitz and I. A. Stegun, *Handbook of Mathematical Functions*. New York: Dover, 1965, p. 447.
[6] K. G. Budden, *Radio Waves in the Ionosphere*. Cambridge, England: Cambridge Univ. Press, 1966.
[7] E. R. Burke and S. M. Bhagat, "The propagation of magnetostatic spin waves in yttrium iron garnet," Univ. of Maryland, College Park, Tech. Rep. 760, 1967.
[8] M. Biri, L. Millanta, N. Rubino, and I. Kaufman, "Magnetostatic waves in axially magnetized cylinders: Experimental dispersion curves," *Nuovo Cimento*, vol. 47B, p. 281, 1967.

Electronic Tuning of the Punch-Through Injection Transit-Time (PITT) Microwave Oscillator

NIZAR B. SULTAN AND G. T. WRIGHT

***Abstract*—Experimental results of the dynamic resistance and capacitance of p⁺-n-p⁺ punch-through injection transit-time (PITT or BARRITT) diodes are presented. A method of predicting the oscillator electronic tuning from the change in the device capacitance is outlined and verified experimentally at *X* band.**

Introduction

Experimental results of the microwave CW performance of the punch-through injection transit-time (PITT) oscillator have been reported recently [1]–[3]. A detailed small-signal design theory has been developed by Wright and Sultan [4] for the device under high-field conditions, taking into account the effects of diffusion and field dependence of carrier mobility. Here we present the experimental results of dynamic capacitance for a p^+-n-p^+ device as a function of frequency and current density. Later, it is shown how these results can be used to predict the performance of the electronic tuning. The latter was investigated at X band in a 7-mm coaxial cavity, and the results are discussed in terms of the change in dynamic capacitance.

Dynamic Impedance

The structure used was a silicon p^+-n-p^+ mesa device, with boron-diffused and evaporated gold contacts, a 4-Ω·cm epitaxial layer, a source to drain spacing of effectively 5 μm, and an active area of 1.2×10^{-4} cm². The devices were mounted in microwave S4 packages [6]. Small-signal measurements of the input impedance for the packaged devices were carried out with a computerized network analyzer. The diode dynamic impedance was deduced from these measurements using an equivalent circuit for the S4 package derived by Owens [5],

Manuscript received March 15, 1972; revised June 26, 1972. This work was supported by the Science Research Council and the Ministry of Technology.

N. B. Sultan was with the Department of Electronic and Electrical Engineering, University of Birmingham, Birmingham, England. He is now at P.O. Box 2771, Damascus, Syria.
G. T. Wright is with the Department of Electronic and Electrical Engineering, University of Birmingham, Birmingham, England.